NOISE CLEANING AND GAUSSIAN MODELING OF SMART PHONE PHOTOPLETHYSMOGRAM TO IMPROVE BLOOD PRESSURE ESTIMATION

Rohan Banerjee, Avik Ghose, Anirban Dutta Choudhury, Aniruddha Sinha and Arpan Pal

Innovation Labs, Tata Consultancy Services Ltd., Kolkata, India

ABSTRACT

Photoplethysmography (PPG) signals, captured using smart phones are generally noisy in nature. Although they have been successfully used to determine heart rate from frequency domain analysis, further indirect markers like blood pressure (BP) require time domain analysis for which the signal needs to be substantially cleaned. In this paper we propose a methodology to clean such noisy PPG signals. Apart from filtering, the proposed approach reduces the baseline drift of PPG signal to near zero. Furthermore it models each cycle of PPG signal as a sum of 2 Gaussian functions which is a novel contribution of the method. We show that, the noise cleaning effect produces better accuracy and consistency in estimating BP, compared to the state of the art method that uses the 2-element Windkessel model on features derived from raw PPG signal, captured from an Android phone.

***Index Terms*—** Photoplethysmography, Blood Pressure, Noise Cleaning, Gaussian Function

1. INTRODUCTION

Smart phone applications for physiological sensing are rapidly gaining popularity in both developed and developing nations. Such applications provide both elderly people and young adults with an opportunity to monitor several physiological vitals regularly at home for indicative and preventive measurements without possessing dedicated clinical devices. Modern smart phones are equipped with a number of inbuilt sensors, including the accelerometer, microphone and camera [1]. Both accelerometer and microphone can be used to measure breathing rate and heart rate, whereas the camera can be used to estimate several vitals using photoplethysmography (PPG) technique.

PPG is a simple non-invasive technique to measure the instantaneous blood flow in capillaries [2]. Capillary blood flow increases during systole and reduces during diastole. Thus, PPG signal of a person is periodic in nature, whose fundamental frequency indicates the heart rate. Researchers have shown that PPG can be a useful technique to measure several physiological vitals including the heart rate (HR) [2], blood pressure (BP), respiratory rate [3], blood oxygen saturation (SpO2) [4] and certain ECG parameters [5]. There is a wide literature available in prior arts, that estimates systolic (P_s) and diastolic (P_d) BP from PPG. Few of them used a combination of PPG and ECG signals for measuring the pulse transit time to estimate BP [6]. PPG signal, synchronized with a microphone [7] can also be used to serve this purpose. Research is also going on to estimate BP, using PPG as the only input source for creating more affordable systems. Teng et al. [8] and Lamonanca et al. [9] proposed a set of time domain PPG features to estimate P_s and P_d using machine learning techniques. In our earlier work [10], we proposed an indirect approach of estimating BP via the R and C parameters of 2-element Windkesel model using PPG features. The proposed approach outperformed [8] and [9] when applied on a benchmark hospital dataset [11].

All the above-mentioned methods perform well when applied on clean and noise-free PPG signals. However, PPG signals, captured using smart phones have several limitations. Smart phones typically capture video at 30 fps, yielding a very low sampling rate of the extracted PPG signal (30 Hz) compared to a clinical pulse-oximeter (100 Hz or more). Ambient lights also affect the signal. A little finger movement or even variation in finger pressure can largely affect the signal quality. All these, make the signal more vulnerable in time domain and less reliable for analysis.

This paper contributes in detail noise cleaning of smart phone PPG signal in terms of 1) reducing baseline drift, 2) modeling PPG signal with a sum of 2 Gaussian functions and 3) removing the outlier PPG features, to obtain more accurate and consistent BP values over [10].

Rest of the paper is organized as follows. Section 2 formulates to estimate BP using 2-element Windkessel model. Section 3 describes the PPG extraction technique from smart phone video. Noise cleaning steps and feature extraction from PPG signals are explained in Section 4 and 5 respectively, followed by experimental results and conclusion sections.

2. ESTIMATION OF BP USING 2-ELEMENT WINDKESSEL MODEL

2-element Windkessel model represents the human cardiovascular system in terms of a resistance (R) and capacitance (C) connected in parallel across an alternative current source ($I(t)$) [12]. R and C represent the peripheral resistance and arterial compliance. The current $I(t)$ denotes the blood flow and the voltage ($P(t)$), across the circuit indicates the resulting blood pressure. Thus the current-voltage relationship becomes:

$$\frac{P(t)}{R} + C\frac{\mathrm{d}P(t)}{\mathrm{d}t} = I(t) \quad (1)$$

The blood flow from ventricles to artery is expressed as a half wave sinusoidal during systole and zero during diastole:

$$I(t) = \begin{cases} I_0 sin(\frac{\pi t}{T_s}), & (n-1)T_c < t \leq (n-1)T_c + T_s \\ 0, & (n-1)T_c + T_s < t \leq nT_c \end{cases} \quad (2)$$

T_s and T_d are the systolic and diastolic time and duration of a cardiac cycle is $T_c = T_s + T_d$. If C_0 be the cardiac output (assumed to be 5 lit/minute for all), I_0 can be solved from Eqn.3 as:

$$\frac{C_0 T_c}{60} = I_0 \int_0^{T_s} sin(\frac{\pi t}{T_s})\mathrm{d}t \quad (3)$$

Putting the two conditions of $I(t)$ in Eqn.1, we can solve for P_s and P_d for a cardiac cycle as:

$$\begin{aligned} P_s &= P(t|t = T_s) \\ &= P_d e^{-T_s/RC} + \frac{I_0 T_s C \pi R^2}{T_s^2 + C^2\pi^2 R^2}(1 + e^{-T_s/RC}) \quad (4) \end{aligned}$$

$$P_d = P(t|t = T_c) = P_s e^{-T_d/RC} \quad (5)$$

As shown in [10], PPG features can be used to estimate R and C parameters using machine learning techniques. However, unlike linear regression in [10], here we use feed forward artificial neural network (ANN) to model the non-linearity between dependent and independent variables. For both R and C, the optimized ANN structures contain a single hidden layer with 15 nodes and a single output node. Tan-Sigmoid activation function is used for the hidden neurons and linear function for the output neurons. PPG features are applied as inputs. Levenberg-Marquardt optimization based back propagation is used to update the weight and bias values of the neurons in training. R and C are calculated from ground truth P_s and P_d. At testing, R and C are estimated from the input PPG features and training models to calculate P_s and P_d.

3. EXTRACTION OF PPG SIGNAL FROM SMART PHONE VIDEO

Smart phones capture PPG signal in reflective mode [13]. The users gently place their fingertip on the smart phone camera with the flash on, to obtain a video sequence of the light reflected from fingertip. Having analyzed the conventional approaches in [13] and [14], we understood that the periodic nature of PPG signal is caused by the varying intensity of redness in the region of interest (ROI) of each video frame. However, Android APIs provide the camera preview information in YC_BC_R colorspace [15]. Thus further conversion to RGB domain in real time causes additional computation in the mobile device, which may reduce the frame rate of the captured video. Since the intensity information is carried in the luminance part of YC_BC_R, we have intuitively used the Y component for PPG extraction. The value of PPG signal corresponding to l^{th} frame of a WXH video segment is calculated as:

$$PPG(l) = \sum_{i=1}^{W}\sum_{j=1}^{H} Y_{i,j}/(W * H) \quad (6)$$

We found that, PPG signal, extracted using the above mentioned technique, produces high correlation coefficient ($R > 0.9$) with the state of the art techniques in [13] and [14].

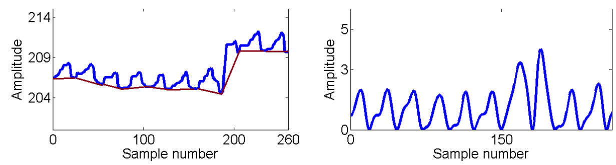

(a) Noisy PPG signal

(b) After pre-processing and removal of baseline drift

Fig. 1. Noise cleaning of PPG signal

4. NOISE CLEANING OF PPG SIGNAL

A typical PPG waveform, captured using Nexus 5 Android phone is shown in Fig 1(a). It can be observed that the signal is too noisy for time domain analysis. Our proposed noise cleaning steps are explained in the following subsections.

4.1. Pre-processing

PPG signal contains a slowly varying DC (due to breathing) and other high frequency noise components. However, the fundamental frequency lies between 1 to 1.5 Hz based on the heart rate of a person (60-90 bpm). Raw PPG signal is shifted to its zero mean and filtered using a 4^{th} order Butterworth band-pass filter having cutoff frequencies of 0.5 Hz and 5 Hz to remove the undesired frequency components.

4.2. Removal of Baseline Drift

Fig. 1(a) shows that PPG signal does not have a fixed baseline. Moreover, both ends of a single PPG cycle are not often aligned. Unequal baseline of PPG signal is a major reason for wrong feature calculation. For a uniformly sampled signal, say F be a vector containing all k samples in one cycle. We construct a second vector T of same length, forming a line segment between the two endpoints of that cycle, with $k-2$ equally spaced values in between, computed using linear interpolation (shown in Fig. 1(a) in red). Then the vector $F^1 = F - T$ represents the modified cycle with zero baseline. The effect of proposed pre-processing and baseline removal algorithm on the entire signal in Fig. 1(a) is shown in Fig. 1(b), making it cleaner for further analysis.

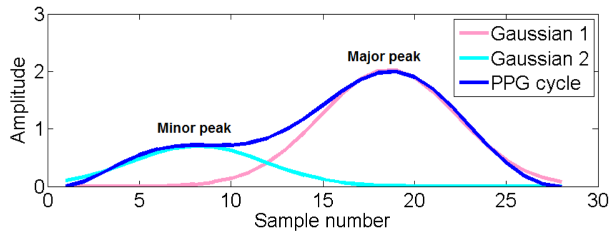

Fig. 2. Modeling of a PPG cycle with a sum of 2 Gaussians

4.3. Modeling of PPG Signal with Sum of 2 Gaussian Functions

As mentioned earlier, PPG signals captured using smart phones are extremely noise-prone and contain several irregularities in shape due to that. Thus, a mathematical modeling can ensure better signal realization for analysis. It is known that, a set of uniformly spaced single valued data can be approximated by a sum of Gaussian functions with good accuracy [16]. Fig. 1(b) shows that a PPG cycle closely follows a Gaussian shape. However it is asymmetric in nature and contains two peaks. The major and prominent peak represents the systolic peak, whereas the minor peak represents the dicrotic peak. Thus, instead of a single Gaussian, a sum of 2 Gaussian functions can aptly fit the shape with better accuracy. If $\{x_k : k = 1, 2....N\}$ be a set of equally spaced data points with corresponding PPG signal value of $\{PPG_k : k = 1, 2, ...N\}$, then our aim is to approximate PPG_k with y_k, as given in Eqn. 7

$$y_k = a_1 e^{\frac{-(k-b_1)^2}{2c_1^2}} + a_2 e^{\frac{-(k-b_2)^2}{2c_2^2}} \quad for\ k = 1, 2, ..N \tag{7}$$

by optimizing the constants $a_1, b_1, c_1, a_2, b_2, c_2$, so that the cost function (h_k) in Eqn.8 gets minimized

$$h_k = \sqrt{\frac{1}{N}\sum_{k=1}^{N}(PPG_k - y_k)^2} \tag{8}$$

An ideal PPG cycle, fitted using a sum of 2 Gaussian curves are shown in Fig. 2. Root Mean Square Error (RMSE) is a popular tool in statistics to measure the goodness of a curve fitting. Typically a lower value indicates a better fitting. The percentage RMSE between the original and modeled cycle in Fig. 2, fitted with 2 Gaussian curves is found to be 1.5%. The same becomes 8.3% and 3.6% respectively, if fitted with a single Gaussian or a Weibull function. For a more comprehensive performance analysis, we consider a PPG waveform, containing different possible shapes of PPG cycle and fit each of them with a sum of 2 Gaussian functions. The actual and modeled waveform are shown in Fig. 3. The percentage RMSE between the actual and modeled signal is computed to be less than 2.5%, indicating the feasibility to fit any kind of PPG waveform with commendable accuracy, The constant a_i indicates the height of the peak, b_i is the position of the center of the peak and c_i controls the width of a Gaussian curve. So we use some of these model parameters as additional PPG features for analysis.

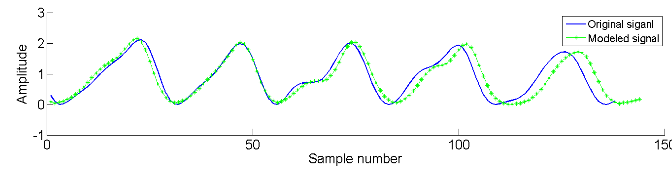

Fig. 3. Modeling of different PPG shapes with 2 Gaussians

5. FEATURE EXTRACTION AND REMOVAL OF OUTLIERS

Our composite feature set includes a combination of features, extracted from each cycle of the original PPG signal as well as the modeled signal. Removal of outlier cycles, caused due to inaccurate detection of troughs is necessary before applying the features to the ANN structures. Input signal is split into rectangular overlapping windows of equal size. If the signal is assumed to be stationary in nature, mean spectral peak location across all the windows indicates its fundamental frequency f_c. So ideal time period becomes $T_{c_{ideal}} = 1/f_c$. Now for all the cycles, we calculate the absolute difference from ideal time period as $\Delta T_c = |T_c - T_{c_{ideal}}|$. A high value of ΔT_c indicates a wrongly detected cycle. K-Means clustering (K=2) [17] is used to remove these outlier cycles. First, histogram analysis is done for all ΔT_c to initialize the cluster centroids, followed by 2-Means clustering and estimating of cluster density to remove the outliers. Centroid of the histogram bin having maximum entries is considered as the initial centroid (C_1) for one cluster. The initial centroid of the other cluster (C_2) is taken as the farthest data point from C_1. K-Means algorithm is used to get the final cluster centroids. Cluster entries corresponding to the centroid with lower Xie-Beni index [18] are considered to be compact and those cycles are used for feature extraction.

Reflective PPG signals are vertically inverted to get the shape of clinical PPG signal [19] before feature extraction. Applying the MIC based feature selection technique, mentioned in [5], we consider the following PPG features in R^7 feature space for estimation of R and C : (1) systolic time (T_s), (2) diastolic time (T_d), (3 and 4) pulse-width at 33% (B_{33}) and 75% (B_{75}) of pulse height respectively, (5) pulse width (T_c) of the original signal (all used in [10]), along with (6) c_1 and (7) c_2 of the fitted Gaussian curves.

6. EXPERIMENTAL SECTION AND RESULTS

Our result section focuses on the improvement achieved over [10], due to noise cleaning, addition of new Gaussian features and ANN based learning, in estimating BP, in terms of accuracy and consistency. Initially, 15 healthy persons, aged

between 30 ± 10 years were selected for creating the training models for R and C. The range of P_s and P_d of the subjects was 120 ± 20 mmHg and 80 ± 10 mmHg respectively. A Nexus 5 Android phone was used for PPG data collection. Ground truth BP was measured using a digital BP measuring device manufactured by Omron [20]. Seated in a complete rest position, fingertip video of each subject was captured at 320x240 resolutions for 45 seconds in average and stored in MP4 format using MPEG-4 video codec. The compressed video was converted to raw YUV video stream using FFmpeg [21], followed by extraction of PPG signal in Matlab. 8 more subjects were chosen for performance evaluation (Testing). 5 sets of video, each having a duration of 30 seconds were collected from every subject with 2 minutes of time gap in between to extract 5 sets of PPG signal. Ground truth BP of all the subjects remained stable during the phase.
Feature extraction and calculation of BP is done on every cycle of the PPG signal. The histogram analysis of P_s and P_d from a single video of a person, having ground truth BP of 115/77 mmHg, obtained using method [10] are shown in Fig. 4(a) and Fig. 4(b) respectively. Fig. 5(a) and Fig. 5(b) shows the histogram of the same person obtained by incorporating the proposed noise cleaning steps. It can be observed that the spread of P_s and P_d across multiple cycles of the same PPG signal is significantly reduces due to noise cleaning. Moreover, it produces more prominent dominant bin in the histogram of both P_s and P_d close to the ground truth value, resulting in better confidence in decision making.

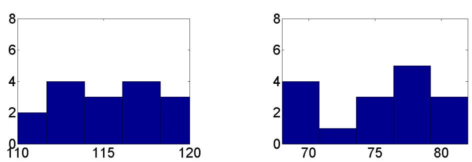

(a) Histogram of P_s in mmHg

(b) Histogram of P_d in mmHg

Fig. 4. Histogram of P_s and P_d using [10]

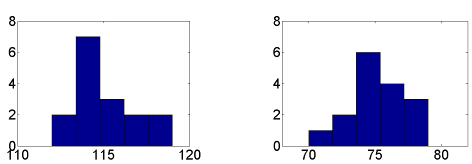

(a) Histogram of P_s in mmHg

(b) Histogram of P_d in mmHg

Fig. 5. Histogram of P_s and P_d after noise cleaning

Table. 1 shows a comparative analysis between [10] and the proposed methodology for all the 8 subjects across all 5 video sessions. As the method in [10] reported to outperform [8] and [9], we exclude them in this paper for performance comparison. For each subject in Table. 1, P_s and P_d are expressed in terms of $mean \pm std$ mmHg over all the cycles of all 5 PPG signals. The gender (M/F) and ground truth BP of each subject are indicated in the first column. PPG signals extracted from subject 3, 4, 7 and 8 were visibly noisier than others due to their finger movement during data collection. The same was reflected in the low PSNR values of their captured videos compared to others. Results show that, incorporating the proposed noise cleaning steps, the estimated mean BP values (both P_s and P_d) for most of the subjects match more closely with the ground truth. Moreover, it invariably decreases the standard deviation in the estimated BP values across multiple video sessions, implying better consistency in the final estimation.
It can be also observed that, subjects having cleaner PPG signals (1, 2, 5, 6), the improvement achieved after noise cleaning is minimal. However for noisy PPG, the proposed noise cleaning effect significantly outperforms [10], justifying its necessity for phone captured noise prone PPG signal.

Table 1. Performance Improvement in Estimating BP over [10] due to Proposed Noise Cleaning

Subject	P_s **in [10]**	P_s **Here**	P_d **in [10]**	P_d **Here**
Sub# 1 (M) 115/77	113 ± 5	114 ± 3	78 ± 7	75 ± 4
Sub# 2 (M) 120/80	118 ± 8	118 ± 6	84 ± 8	82 ± 5
Sub# 3 (M) 125/84	112 ± 8	119 ± 8	65 ± 13	76 ± 6
Sub # 4 (M) 135/85	121 ± 8	128 ± 6	73 ± 8	79 ± 6
Sub # 5 (F) 90/60	97 ± 4	95 ± 2	65 ± 6	62 ± 6
Sub# 6 (F) 120/80	119 ± 4	119 ± 4	76 ± 6	77 ± 4
Sub# 7 (F) 120/82	110 ± 9	115 ± 3	68 ± 11	75 ± 6
Sub# 8 (F) 130/80	119 ± 10	125 ± 5	88 ± 13	84 ± 4

7. CONCLUSION

The present work deals with noise cleaning and mathematical modeling of smart phone captured PPG signal for estimation of BP. The proposed methodology produces improved accuracy and better consistency even on noisy PPG signal. However, it needs to be successfully tested on larger and demographically diverse dataset. Our future works include performance evaluation of the proposed noise cleaning algorithms on PPG signal, captured using low cost smart phones as well as creating generic training models that can work regardless the hardware configuration. We are also exploring the feasibility of including person specific modeling for further improvement in estimation.

8. REFERENCES

[1] "Sensors in smart phones," `http://web.stanford.edu/class/cs75n/Sensors.pdf`, [Online; accessed 5th October-2014].

[2] J. Allen, "Photoplethysmography and its application in clinical physiological measurement," *Physiological Measurement*, vol. 28, 2007.

[3] D. J. Meredith, D. Clifton., P. Charlton, J. Brooks, C.W. Pugh, and L. Tarassenko, "Photoplethysmographic derivation of respiratory rate: a review of relevant physiology," *Journal of Medical Engineering and Technology*, vol. 36, no. 1, January 2012.

[4] Gilwon Yoon, Jong Y. Lee, Kye Jin Jeon, Kun-Kook Park, Hyung S. Yeo, Hyun T. Hwang, Hong S. Kim, and In-Duk Hwang, "Multiple diagnosis based on photoplethysmography: hematocrit, spo2, pulse, and respiration," 2002.

[5] Rohan Banerjee, Aniruddha Sinha, Anirban Dutta Choudhury, and Aishwarya Visvanathan, "PhotoECG: photoplethysmography to estimate ECG parameters," in *ICASSP2014 - Bio Imaging and Signal Processing (ICASSP2014 - BISP)*, Florence, Italy, May 2014, pp. 4437–4441.

[6] J. M. Zhang, P.F. Wei, and Y. Li, "A labview based measure system for pulse wave transit time," in *International Conference on Information Technology and Applications in Biomedicine*, 2008, pp. 177–480.

[7] V. Chandrasekaran, R. Dantu, S. Jonnada, S. Thiyagaraja, and K.P. Subbu, "Ieee transactions on biomedical engineering," *Physiological Measurement*, vol. 60, no. 4, pp. 1080–1089, APRIL 2013.

[8] XF Teng and YT Zhang, "Continuous and noninvasive estimation of arterial blood pressure using a photoplethysmographic approach," in *Engineering in Medicine and Biology Society, 2003. Proceedings of the 25th Annual International Conference of the IEEE*. IEEE, 2003, vol. 4, pp. 3153–3156.

[9] Francesco Lamonaca, Kurt Barbe, Yuriy Kurylyak, Domenico Grimaldi, Wendy Van Moer, Angelo Furfaro, and Vitaliano Spagnuolo, "Application of the artificial neural network for blood pressure evaluation with smartphones," in *Intelligent Data Acquisition and Advanced Computing Systems (IDAACS), 2013 IEEE 7th International Conference on*. IEEE, 2013, vol. 1, pp. 408–412.

[10] AD Choudhury, R Banerjee, A Sinha, and S Kundu, "Estimating blood pressure using windkessel model on photoplethysmogram," in *Engineering in Medicine and Biology Society, 2014. Proceedings of the 36th Annual International Conference of the IEEE*. IEEE, 2014.

[11] Liu D, Grges M, and Jenkins SA, "University of queensland vital signs dataset: development of an accessible repository of anesthesia patient monitoring data for research," *Anesth Analg*, vol. 114, no. 3, March 2012.

[12] Westerhof N., Lankhaar J.W., and Westerhof B.E., "The arterial windkessel," *Med Biol Eng Comput.*, vol. 47, no. 2, February 2009.

[13] Yu. Kurylyak, F. Lamonaca, and D. Grimaldi, "Smartphone-based photoplethysmogram measurement," *in Digital Image, Signal and Data Processing for Measurement Systems, R.J. Duro and F. Lpez-Pea Ed*, pp. 135–164, 2012.

[14] A. Pal, A. Sinha, A.D. Choudhury, T. Chattopadhyay, and A. Visvanathan, "A robust heart rate detection using smart-phone video," in *MobileHealth Workshop in MobiHoc*, 2013.

[15] "Android camera api," `http://developer.android.com/reference/android/hardware/Camera.html`, [Online; accessed 5th October-2014].

[16] A. Goshtasby and W.D. Oneill, "Curve fitting by a sum of gaussians," *CVGIP: Graphical Models and Image Processing*, vol. 56, no. 47, 1994.

[17] F. Rehm, F. Klawonn, and R. Kruse, "A novel approach to noise clustering for outlier detection," *Soft Comput.*, vol. 11, no. 5, pp. 489–494, December 2006.

[18] Xuanli Lisa Xie and G. Beni, "A validity measure for fuzzy clustering," *Pattern Analysis and Machine Intelligence, IEEE Transactions on*, vol. 13, no. 8, pp. 841–847, 1991.

[19] J. Nijboer, J. Dorlas, and H. Mahieu., "Photoelectric plethysmography: Some fundamental aspects of the reflection and transmission method," *Clinical Physics and Physiological Measurement*, vol. 2, no. 3, pp. 205–215, 1981.

[20] "Omron blood pressure monitors," `http://omronhealthcare.com/home-products/blood-pressure-monitors/`, [Online; accessed 5th October-2014].

[21] "Ffmpeg," `https://www.ffmpeg.org/about.html`, [Online; accessed 5th October-2014].